Scientific Research and Essays Vol. 7(33), pp. 2983-2991, 23 August, 2012
Available online at http://www.academicjournals.org/SRE
DOI: 10.5897/SRE12.042
ISSN 1992-2248 ©2012 Academic Journals

Full Length Research Paper

Impaired N-cadherin-mediated adhesion increases the risk of inducible ventricular arrhythmias in isolated rat hearts

Hong-jun Zhu[1], Xiao-Mei Ding[1], Jian-gang Zou[2]*, Xiao-feng Hou[2] and Ke-jiang Cao[2]

[1]Department of Cardiology, Anhui Provincial Hospital, 17 Lujiang Road, Hefei, Anhui Province, 230001, China.
[2]Department of Cardiology, First Affiliated Hospital of Nanjing Medical University, 300 Guangzhou Road, Nanjing, Jiangsu Province, 210029, China.

Accepted 16 July, 2012

Recent studies suggest that cadherin-mediated adherens junctions may be impaired in diseases and pathologic processes related to ventricular arrhythmias, which are concomitant with decreased connexin 43 (Cx43). In this study, we evaluated the acute arrhythmogenic effects of adherens junction impairment in isolated rat hearts. A total of 56 hearts isolated from adult male rats were perfused with 0.2 mM AHAVD, a synthetic peptide that specifically inhibits N-cadherin (n = 18); 0.2 mM IPPINL, a nonsense peptidase that contains the highly conserved cadherin sequence (n = 18), and oxygenated Krebs–Henseleit buffer as the control (n = 20). Under programmed stimuli, ventricular tachyarrhythmias were induced more in the AHAVD-perfused hearts (9/18) than the IPPINL-perfused hearts (4/18) and those in the control (3/20) group ($P < 0.05$). The conduction velocity of the left ventricular myocardium exhibited an inverse pattern in these three groups (53.5 ± 6.3 cm/s, 65.2 ± 6.2 cm/s, and 66.3 ± 8.8 cm/s, respectively, $P < 0.05$). The effective refractory period and the epicardial action potential duration at 90% repolarization were not significantly different among the groups after 1 h of perfusion. Cx43 redistribution and PS368 decrease was observed in the AHAVD-perfused heart tissues. The reduction in functional GJs in the intercalated discs of cardiomyocytes may be one of the initial mechanisms by which myocardial conduction is blunted. Furthermore, rat hearts with impaired adherens junctions are more susceptible to ventricular tachyarrhythmias.

Key words: Adherens junctions, N-cadherin, connexin 43, pS368, Ventricular tachyarrhythmia.

INTRODUCTION

N-cadherin (N-cad) is an important transmembrane component of adherens junctions through its extracellular amino terminal region and it forms homophilic adhesions among neighboring cells. N-cad–mediated adherens junctions stabilize the plasma membranes of adjacent cardiomyocytes to help form an environment suitable for the formation and maintenance of large arrays of electrical channels known as gap junctions (GJs) (Li et al., 2006). GJs are composed of connexins, which are highly homologous proteins that facilitate direct communication and form low-resistance channels between adjacent cells by allowing the passage of ions and small metabolites (Sohl and Willecke, 2004; Harris, 2007). Connexin 43 (Cx43) is the most prominent protein subunit of connexins in the ventricular myocardium of all mammalian species. Altered Cx43 expression or distribution and Cx43 phosphorylation have been shown to impair the propagation of electrical impulses and promote arrhythmias during ischemia–reperfusion injury, heart failure, arrhythmogenic right ventricular cardiomyopathy (ARVC), and other pathologic conditions

*Corresponding author. E-mail: jgzou@njmu.edu.cn. Tel: +86 25 8481 8007. Fax: +86 25 8367 4357.

that accompany high risk of ventricular arrhythmias (Kaplan et al., 2004; Poelzing and Rosenbaum, 2004; Sato et al., 2008). Recent studies confirm that severe conduction defects and increased susceptibility to ventricular tachyarrhythmias (VTs) are associated with the GJ remodeling that result from the cardiac-specific deletion of N-cad (Li et al., 2008). Cell adhesion is also disturbed under certain pathologic conditions such as healed infarcts and several subtypes of arrhythmogenic right ventricular cardiomyopathy (ARVC), wherein mutations in desmosomal cadherins were found (Pilichou et al., 2006; van den Borne et al., 2008). Each condition is associated with a high risk of lethal ventricular arrhythmias and GJ remodeling. However, the initial effects of adherens dysfunction on GJ remodeling and the increase in ventricular arrhythmias remain unclear.

In our previous studies, we proved that AHAVD, a synthetic peptide that specifically inhibits the homophilic binding of N-cadherin, inhibits N-cadherin–mediated cell–cell adhesion and rapidly results in Cx43 redistribution and serine368 dephosphorylation. This inhibition results in impaired GJ communication between cardiomyocytes (Zhu et al., 2010). We hypothesize that impaired N-cadherin–mediated adhesion also affects GJ conduction and increases susceptibility to ventricular arrhythmias.

In the present study, AHAVD (the synthetic peptide sequence Ala-His-Ala-Val-Asp-NH_2) was introduced as a selective inhibitor of N-cad–mediated adhesion. Impaired cell–cell adhesion acutely affected the electrical channels in isolated adult rat hearts. The electrical properties and conductivity of the left ventricular myocardium were analyzed by using monophasic action potentials (MAPs) and the risk of inducible arrhythmias was evaluated electrophysiologically. Our findings indicate that AHAVD impairs N-cad–mediated cell–cell adhesion, which results in Cx43 redistribution and pS368 dephosphorylation, reduces the conduction velocity of the myocardium, and increases the risk of inducible ventricular arrhythmias.

MATERIALS AND METHODS

The study was performed in accordance with the Guide for the Care and Use of Laboratory Animals (NIH Publication No. 85-23, National Academy Press, Washington, DC, revised 1996). The experimental protocol was approved by the Animal Care and Use Committee of Nanjing Medical University. Adult (16 to 20 weeks old) male Sprague–Dawley rats were provided by the Animal Research Center of Nanjing Medical University (Nanjing, China). All adult rats were housed at a constant temperature (23 ± 2°C) and humidity (70 ± 5%) under a 12 h light/dark cycle. They were provided a standard diet during an acclimation period of at least two days.

Isolation of rat hearts

The rats were anesthetized with pentobarbital (70 mg/kg) and their hearts were then excised rapidly and placed in oxygenated Krebs-Henseleit buffer (118.3 mM NaCl, 2.7 mM KCl, 1.0 mM $MgSO_4$, 1.4 mM KH_2PO_4, 29.0 mM $NaHCO_3$, 3.4 mM $CaCl_2$, and 10 mM glucose, plus insulin 70 mU/L and 2.8% bovine serum albumin, pH 7.4) at 37°C using a Langendorff perfusion device, as previously described (Lerner et al., 2000). The hearts were perfused via retrograde aortic flow with Krebs–Henseleit buffer at 37°C. The flow rates were adjusted to maintain a constant perfusion rate of 7 ml/min. The hearts were immersed simultaneously in a bath that contains oxygenated buffer at 37°C to maintain a constant temperature. Any heart that exhibited contractile dysfunction or other evidence of injury was discarded during the initial 20 min equilibration period. The hearts were randomly assigned to three groups and studied after the equilibration period. The AHAVD-perfused group (n = 18) was perfused with 0.2 mM AHAVD/perfusion buffer, as the negative control, the IPPINL (Ile-Pro-Pro-Ile-Asn-Leu-NH_2, a nonsense peptidase that contains the highly conserved cadherin sequence) was perfused with 0.2 mM IPPINL/perfusion buffer (n = 18), and the control hearts (n = 20) were perfused with oxygenated buffer.

Transmission electron microscopy

The left ventricular myocardia from four hearts in each group were cut into 1 mm^3 sections. After overnight fixation in 3% glutaraldehyde, the small tissue samples were embedded in Epon by following routine procedures. Ultrathin sections were stained with uranyl acetate and lead citrate, and were then viewed and photographed under a Philips EM-400 electron microscope.

Immunofluorescence labeling

Flash-frozen sections of four hearts in each group were fixed with 4% paraformaldehyde. The sections were incubated overnight with mouse monoclonal anti-Cx43 antibodies (ab79010, Abcam, Cambridge, UK) and rabbit polyclonal anti-pS368 antibodies (sc-101660, Santa Cruz Biotechnology, USA) at 4°C. Then, the sections were incubated at 37°C for 1 h with rhodamine-conjugated goat anti-rabbit and FITC-conjugated goat anti-mouse secondary antibodies. The double-stained sections were observed and the immunofluorescence signals specific to Cx43 and pS368 were examined under confocal immunofluorescence microscopy (Zeiss LSM510 META, Germany). The images were then digitized into 1024 × 1024 matrices.

Monophasic action potentials (MAPs) recordings and programmed electrical stimulation

The MAPs of the left ventricular epicardia were recorded after the 20 min stabilization interval and at 15, 30, 45, and 60 min time points during the succeeding 60 min perfusion period using an Ag-Cl contact electrode (0.25 mm tip diameter). A bipolar pacing electrode was placed near the apex of the heart on the anterior epicardial surface of the right ventricle. The pacing protocols used 2 ms square-wave stimuli with amplitudes three times higher than the excitation threshold. A programmed electrical stimulus was introduced to measure the effective refractory period (ERP), as previously described (Thomas et al., 2008). To induce ventricular tachycardia (VT), burst pacing (18 S1 stimuli) was performed as in the previously described protocol (Betsuyaku et al., 2004). The electronically stored traces were recorded and analyzed using an RM6240 B/C physiologic signal handling system 2.0 (Chengdu Instrument Corp, Chengdu, China). The point of maximum positive deflection was considered the point of 0% repolarization, and the return to baseline was the point of 100% repolarization. The epicardial action potential duration at 90% repolarization (APD90) was measured to compare MAP durations among the groups. All

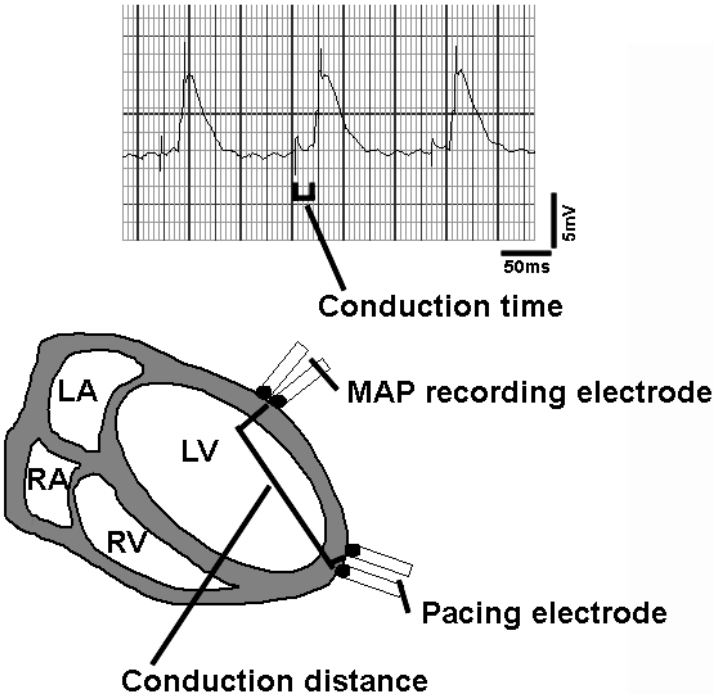

Figure 1. MAP recording and measurement of conduction velocity. Schematic drawing of the stimulation and recording sites for the conduction velocity measurement.

recordings were performed at steady-state pacing of 130 ms to negate rate-dependent differences in action potential duration (APD).

Conduction velocity

The conduction velocity on the anterior LV wall of six hearts from each group was measured at 0, 15, 30, 45, and 60 min of perfusion during ventricular pacing at a cycle length of 130 ms, as described in previous literature (Kamei et al., 2007). Two platinum stimulating electrodes were inserted 2 mm apart at the LV apex of the isolated hearts during the 60 min perfusion period. An AgCl contact (0.25 mm tip diameter) MAP electrode was positioned on the epicardium near the center of the LV anterior wall. The time from the pacing electrodes to MAP onset was defined as the conduction time. The length of the epicardial surface from the pacing site to the MAP recording site was measured using a graduated copper wire, and the conduction velocity was calculated as distance/conduction time (cm/s) (Figure 1).

Immunoblotting

The total N-cadherin and the Cx43 content were detected by immunoblotting, as previously described (Johnson et al., 2002; Nakao et al., 2008). Lysates of heart tissues were centrifuged and the proteins were eluted by boiling for 10 min in sodium dodecyl sulfate (SDS) sample buffer (0.25 M Tris-HCl, pH 6.8, 4% SDS, 40% glycerol, and 0.002% bromophenol blue). Aliquots of the proteins were resolved in 10% polyacrylamide gel via SDS polyacrylamide gel electrophoresis and transferred (semi-dry) onto nitrocellulose membranes. The membranes were blocked for 2 h in 5% nonfat dry milk in Tris-buffered saline–Tween-20 at room temperature, and then incubated overnight with rabbit anti-Cx43 (1:4000), rabbit anti-phosphorylated-Cx43 (1:2000), mouse anti-Glyceraldehyde 3-phosphate dehydrogenase (GADPH) (1:4000), rabbit anti-N-cadherin (1:2000), and mouse anti-N-cadherin (1:2000) antibodies at 4°C. Horseradish peroxidase (HRP)-conjugated goat anti-mouse and anti-rabbit were used as secondary antibodies. GAPDH was used as the protein loading marker. The densities of the individual bands were quantified as ratios to that of GAPDH.

Statistical analyses

All data are expressed as mean ± SD. The incidences and frequencies of inducible VT in the AHAVD- and the IPPINL-perfused groups were compared with those of the control hearts using a Fisher's exact test. The time of onset of the first run of VT was analyzed by the Kaplan–Meier method. Differences with $P < 0.05$ were considered significant.

RESULTS

AHAVD disrupts cell–cell adhesion and results in Cx43 redistribution in isolated perfused rat hearts

To determine the effects of impairing adherent junctions with AHAVD, transmission electron microscopy was performed on four hearts from the AHAVD-perfused, the IPPINL-perfused, and the control groups. Ultrastructural analysis showed that the AHAVD-perfused, IPPINL-perfused, and control hearts exhibited well-organized

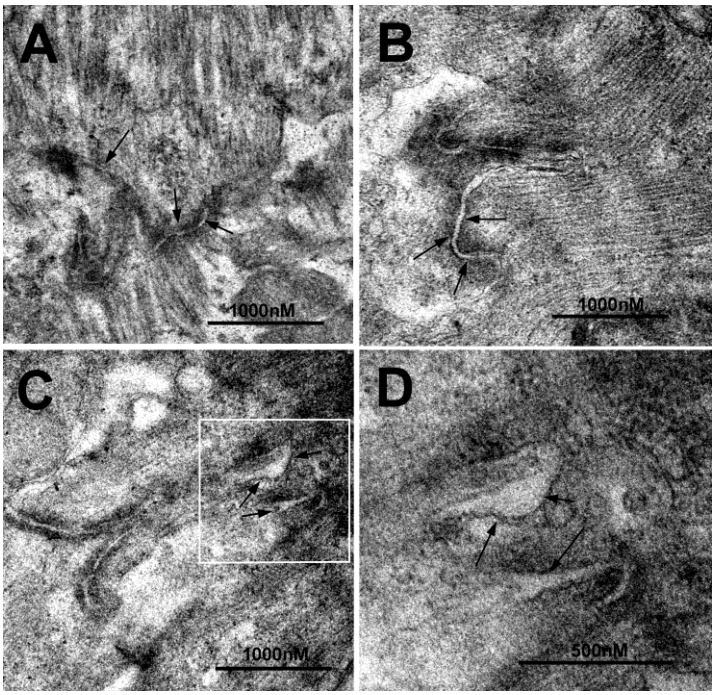

Figure 2. Ultrastructure of the isolated perfused hearts. A and B typical electron microscopy image of tissue sections from control and IPPINL-perfused groups. The image shows a regular membrane (marked by arrows) and intercalated disks between adjacent cardiomyocytes (×30000 original magnification). C. Widened gap of fascia adherens (arrows) in tissue sections from AHAVD-perfused hearts (×30000 original magnification). D. Magnified view of the frame in panel C (×30000 original magnification).

myofibrils with clearly defined Z bands (Figure 2). The intercalated discs of the IPPINL-perfused and control hearts were well formed and the insertion of the myofibrils in the adherens junction appeared normal. However, the gaps between the fascia adherens were widened in the AHAVD-perfused hearts, which may indicate impaired adherens junctions.

The flash-frozen tissue sections from four hearts in each group were double-labeled for Cx43 and pS368 and were inspected under laser confocal microscopy. In both groups, most of the pS368 signals were localized tip to tip in the IC discs; only a few signals were distributed bilaterally in the cells. The intensity of the pS368 signals decreased significantly in the AHAVD-perfused hearts, whereas the intensity of the Cx43 signals did not decrease in the AHAVD perfused hearts. However, significant side distributions of Cx43 signals were apparent in tissues from the AHAVD-perfused hearts (Figure 3).

To understand further the effect of impaired N-cad–mediated adhesions on Cx43-containing gap junctions, the total Cx43 and pS368 in four hearts from each group were measured by immunoblotting (Figure 4). Compared with the control and IPPINL-perfused hearts, the total Cx43 protein in the AHAVD-perfused hearts did not change significantly at each concentration. However, a significant reduction in pS368 was seen in the hearts perfused with 0.2 mM AHAVD (0.24 ± 0.05) compared with the control hearts (0.43 ± 0.07, $p < 0.05$). Given the immunofluorescence and immunoblot results, inhibiting N-cadherin–mediated adhesion using AHAVD was expected to impair GJ conduction function.

Electrical properties and conduction velocity of AHAVD-perfused hearts

All 20 controls (not subjected to polypeptides) remained in sinus rhythm and contracted vigorously throughout the 60 min perfusion period. No runs of spontaneous VT occurred in the control hearts. Electrical activities of the isolated perfused rat hearts in the control group remained relatively stable throughout the 60 min oxygenated perfusion period. The ERP, APD90, and ERP/APD90 of the AHAVD-perfused hearts did not show any difference at any time point when compared with the control and IPPINL-perfused hearts (Table 1). One of the AHAVD-perfused hearts experienced a round of spontaneous VT (non-sustained VT, <3 s) during the 60 min perfusion period.

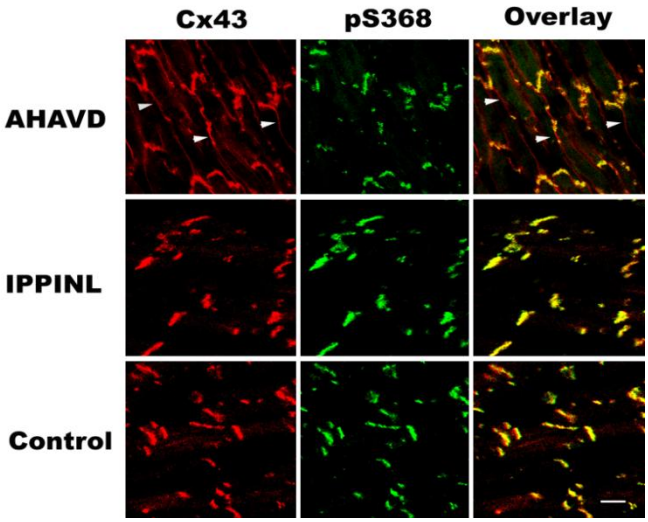

Figure 3. AHAVD affects the distribution and phosphorylation of Cx43 at S368 in the isolated rat hearts. Typical immunofluorescence images from the AHAVD- and IPPINL-perfused rat hearts and oxygenated K–H buffer-perfused hearts. Double-labeling with N-cadherin (green) and Cx43 (red) that shows dose-related Cx43 redistribution to the bilateral edges of cardiomyocytes (arrowheads) in the AHAVD-perfused heart tissue (bar = 20 μm for all panels).

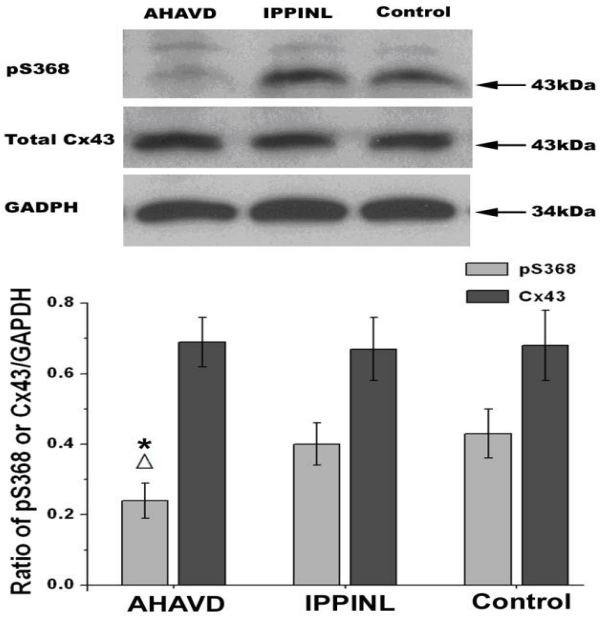

Figure 4. Immunoblot analysis of the total Cx43 and pS368 in AHAVD-perfused hearts. A. Representative immunoblot of total Cx43 and pS368 from the hearts of the control group, the 0.2 mM AHAVD-perfused group, and the 0.2 mM IPPINL-perfused group. GADPH was used as the loading control. B. Densitometric scanning of the total Cx43 and pS368 in the rat hearts (n = 4, each group). Quantitative analysis showed significant reduction of pS368 in the hearts perfused with 0.2 mM AHAVD (* $P < 0.05$, compared with control, △ $P < 0.05$, compared with IPPINL group).

Table 1. Comparison of the ERP and the APD90 of the AHDVD-perfused, IPPINL-perfused, and control groups.

	Time point of perfusion (min)				
	0	**15**	**30**	**45**	**60**
Control (n = 20)					
ERP (ms)	38 ± 8.5	38 ± 8.3	39 ± 7.2	39 ± 8.1	40 ± 8.7
APD90 (ms)	54 ± 7.5	54 ± 7.8	56 ± 8.4	58 ± 8.3	58 ± 8.9
ERP/APD90	0.72 ± 0.16	0.71 ± 0.17	0.69 ± 0.18	0.69 ± 0.20	0.68 ± 0.18
IPPINL-perfused (n = 18)					
ERP (ms)	38 ± 7.8	38 ± 8.6	39 ± 8.2	39 ± 8.4	39 ± 8.7
APD90 (ms)	53 ± 7.5	54 ± 7.8	56 ± 7.9	56 ± 8.2	57 ± 7.8
ERP/APD90	0.73 ± 0.20	0.71 ± 0.16	0.68 ± 0.21	0.67 ± 0.18	0.67 ± 0.19
AHAVD-perfused (n = 16)					
ERP (ms)	38 ± 8.3	38 ± 8.7	39 ± 8.5	41 ± 8.6	42 ± 8.9
APD90 (ms)	54 ± 7.6	55 ± 7.8	57 ± 8.2	59 ± 8.7	61 ± 8.7
ERP/APD90	0.72 ± 0.16	0.70 ± 0.18	0.69 ± 0.17	0.68 ± 0.19	0.68 ± 0.22

ERP = Effective refractory period, APD90 = action potential duration at 90% repolarization.

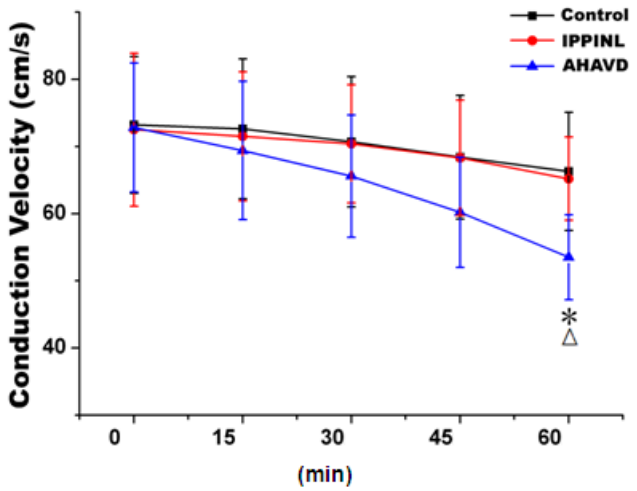

Figure 5. Reduction in conduction velocity of AHAVD-perfused hearts. Line charts of the changes in conduction velocity in the AHAVD-perfused, IPPINL-perfused, and control groups (n = 6, each group), which show a significant reduction in conduction velocity in AHAVD-perfused hearts compared with the control group after 60 min perfusion. (* $P < 0.05$, compared with control,△ $P < 0.05$, compared with IPPINL group).

The conduction velocity was studied every 15 min during perfusion of six hearts from each group. The conduction velocity of the AHAVD-perfused group at the beginning of perfusion was 72.8 ± 9.6 cm/s, which is similar to that of the IPPINL-perfused group and the control group (72.5 ± 10.4 cm/s and 73.2 ± 10.2 cm/s, respectively). However, the conduction velocity in the AHAVD-perfused group showed a time-dependent decrease and was significantly slower after 60 min perfusion than the control group [53.5 ± 6.3 and 66.3 ± 8.8 cm/s respectively, $P < 0.05$ (Figure 5)]. While no deference between the IPPINL-perfused group (64.2 ± 8.2 cm/s) and the control group was observed.

AHAVD increases the susceptibility of isolated rat hearts to ventricular arrhythmias

VTs were induced in each of the three groups using

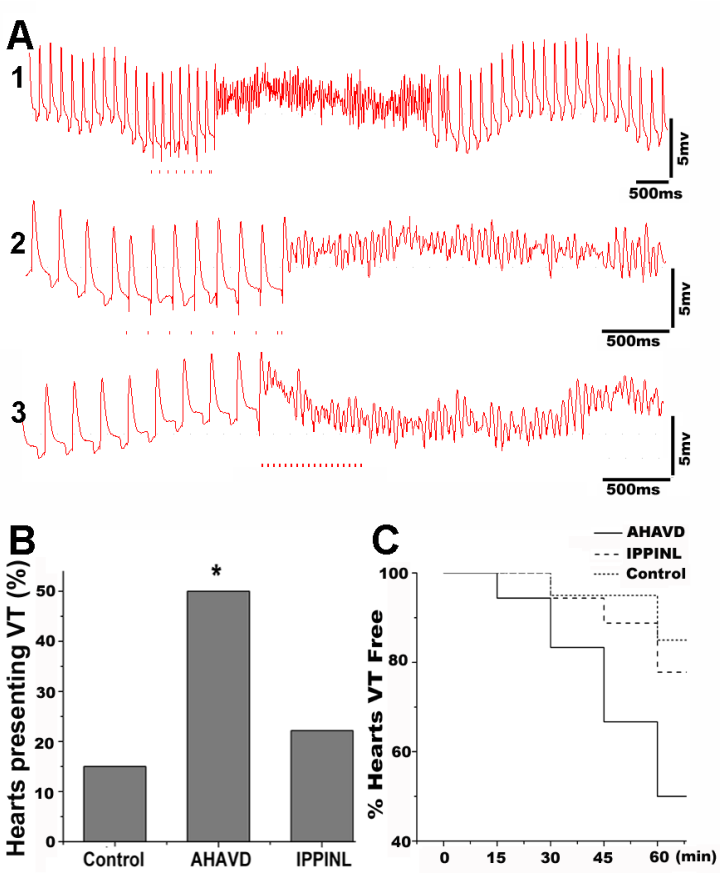

Figure 6. Occurrence of Induced VTs in Isolated Rat Hearts. A. Recorded MAPs with examples of the types of arrhythmias observed after AHAVD perfusion. 1. A brief run of non-sustained VT induced by S1S2 stimuli at 25 ms S1S2 intervals. 2. A run of sustained VT induced by S1S2 stimuli at 35 ms S1S2 intervals. 3. A run of sustained VT induced by 18 S1 stimuli at a cycle length of 25 ms. B. Proportion of induced VT in the groups. * $P < 0.05$ by x^2 analysis. C. Onset of induced VTs in the AHAVD-perfused, IPPINL-perfused, and control hearts during 1 h perfusion.

programmed stimulation (Figure 6A). Non-sustained VTs were observed in 2 of the 20 hearts from the control animals and only one heart developed sustained VT. In the AHAVD-perfused group, induced VT was observed in 9 of the 18 hearts (7 sustained and 2 non-sustained). The proportion of inducible VT was significantly greater in the AHAVD-perfused hearts ($P < 0.05$). In addition, the multiple runs of VT were induced in the AHAVD-perfused group. Sustained VTs were observed in 2 of the 18 IPPINL-perfused hearts and non-sustained VTs were induced in 2 hearts (Figure 6B). The Kaplan–Meier plot shows the time of onset of the first run of VT (Figure 6C). The AHAVD-perfused hearts exhibited an increasing trend towards inducible VTs.

DISCUSSION

We studied the initial effect of impaired adherens junctions between cardiomyocytes on GJs, the most important electrical connections. In this study, we introduced the synthetic peptide AHAVD to inhibit N-cad–mediated adhesion and detected its efficiency in impairing the adherens junctions in isolated rat hearts. Prompt side distribution of Cx43 accompanied by the loss of phosphorylated pS368 in the IC discs was observed. When the N-cad–mediated adherens junctions were impaired by AHAVD, the redistribution of dephosphorylated Cx43 at S368 in the isolated hearts was accompanied by increased susceptibility to induced arrhythmias.

N-cad fortifies adherens junctions to provide strong cell–cell adhesion, which is important in the formation and maintenance of GJs in cardiomyocytes (Li et al., 2006; Noorman et al., 2009). It also links to actin cytoskeleton via the cadherin/catenin complex, which is essential in maintaining the structural integrity of the

heart (Kostetskii et al., 2005). Impaired adherens junctions in both disease states and animal models are associated with GJ remodeling and a high risk of ventricular arrhythmias (Ferreira-Cornwell et al., 2002; Kaplan, 2004; Li et al., 2008). However, the initial effects of impaired N-cad-mediated adhesion remain unclear. Previous studies report that gap junctions may be insufficient for stabilizing larger Cx43 plaques in heterozygous mice with reduced N-cadherin expression although the total number of plaques was unaffected (Li et al., 2008).

The inherent instability of Cx43, as indicated by the 1 h to 2 h turnover rate in the intact heart (Beardslee et al., 1998; Segretain and Falk, 2004), may largely account for their instability in diseased myocardium. A previous study demonstrated that the prompt and retrievable internalization of Cx43 in cultured adult rat cardiomyocytes when the N-cad–mediated adhesion was impaired by removing Ca^{2+} from the culture medium (Hertig et al., 1996). Similarly, the Cx43 in the IC discs of the isolated AHAVD-perfused rat hearts was rapidly redistributed onto the bilateral membrane of cardiomyocytes. The results of the present study confirm the importance of N-cad–mediated adhesion for maintaining GJs and imply that impaired N-cad–mediated adhesion influences GJ function.

At present, information regarding the effects of reduced N-cadherin on the gap junctions in diseased human myocardia is limited. However, impaired adherens junctions were observed in the hearts of patients who suffered from ARVC (Pilichou et al., 2006). Abnormal interstitial cystitis (IC) disc structures, which are associated with N-cadherin and Cx43 downregulation, were observed in a hereditary hamster model of dilated cardiomyopathy (Luque et al., 1994; Fujio et al., 1995). In the present study, we observed significant Cx43 redistribution and reduced pS368 phosphorylation in the heart tissues when N-cad–mediated adhesion was impaired with AHAVD. This may reflect accelerated loss of functional GJs in response to adherens junction impairment.

Impaired electric coupling of GJs causes conduction disturbances and arrhythmia (Lerner et al., 2000; Gutstein et al., 2001). In the present study, the conduction ability of cardiomyocytes was also examined to determine whether impaired adherens junctions affect the electrical coupling of GJs. Although previous mapping analysis can accurately determine conduction velocity, in the current study, conduction velocity is defined as the time from the pacing electrode to the MAP onset between the center of LV anterior wall and apex (Ciaccio, 2000). We found that the conduction velocity of the left ventricular myocardium decreased significantly in the AHAVD-perfused hearts concomitant with the redistribution of Cx43. We also reported arrhythmogenic effects of impaired N-cad–mediated adherens junctions by treating the isolated rat hearts with AHAVD. An EPS was performed to determine whether impaired fascia adherens and the consequent changes in Cx43 are correlated with susceptibility to ventricular arrhythmias. The results show a significantly increased incidence of induced ventricular arrhythmias in the AHAVD-perfused hearts.

Cx43 reduction reportedly results in slower conduction and enhances the development of stable reentrant circuits, which is a major mechanism underlying the occurrence of ventricular tachyarrhythmias in related diseases. Previous studies demonstrated that Cx43 suppression must be at least 80% to change the conduction velocity in otherwise healthy tissues (van Rijen et al., 2004). However, Li et al. (2008) reported that a 40% reduction in Cx43 sufficiently slows down ventricular conduction to cause ventricular arrhythmias and sudden death in N-cad conditional knockout mice (Li et al., 2008). Cx43 is a multi-phosphorylated protein. The phosphorylation/dephosphorylation of Cx43 regulates the internalization, degradation and channel-gating properties of GJs. It was reported in previous study that phosphorylation of serine 368 (S368) is required for mediated reduction in channel conductance (Cottrell et al., 2001; Ek-Vitorin et al., 2006). In the present study, rapid Cx43 redistribution and pS368 dephosphorylation were observed and the electrical conduction function of the GJs was depressed in the AHAVD-perfused rat hearts. Although a reduction in conduction velocity alone is unlikely to increase arrhythmogenicity significantly, it may demonstrate the importance of N-cad–mediated adhesion in maintaining the electrical coupling between cardiomyocytes.

The IC disc is functionally far more complex than a mere junction. Numerous ion channels are located in the IC discs. A previous study on *Xenopus laevis* oocytes show that Kv1.5 channel activity is affected by N-cad expression (Koutsouki et al., 2007). N-cad also reportedly modulates high-threshold voltage-activated calcium channels through the juxtamembrane domain in chick ciliary neurons (Piccoli et al., 2004). Both Kv1.5 and voltage-activated calcium channels are instrumental in the repolarization of cardiomyocytes. Deregulation of these ion channels reportedly correlates with ventricular arrhythmias. In the present study, ERP and APD90 were slightly prolonged in the AHAVD-perfused and control hearts after 1 h perfusion. However, no significant difference was observed between the groups. Based on these results, AHAVD is not likely to increase the risk of arrhythmogenesis via its influence on the ion channels. Further investigations are necessary to determine the link between N-cad and ion channels in cardiomyocytes to elucidate the arrhythmogenic effect of adherens junction dysfunction.

CONCLUSIONS AND CLINICAL IMPLICATIONS

In summary, the peptide AHAVD acutely interrupts N-

cad–mediated adhesion, which results in rapid Cx43 redistribution and reduced conduction velocity in isolated rat hearts. The incidence of inducible arrhythmias was increased in AHAVD-perfused hearts. The results of our study demonstrate the importance of mechanical coupling between cardiomyocytes in maintaining electrical coupling. The present study also shows that the loss of large arrays of GJs may be one of the initial arrhythmogenic mechanisms in diseases that involve impaired mechanical coupling. Investigations on the effect of adherens junction impairment on electrical coupling may shed new light on the mechanism of arrhythmias.

Interventions that enhance cardiac cell adhesion may help maintain the quantity and function of GJs in IC discs. Further investigations of the relationship between mechanical and electrical couplings under pathologic conditions are required to elucidate the potential benefits of enhancing mechanical connections for preventing lethal ventricular arrhythmias.

ACKNOWLEDGMENTS

This work was supported by a grant from the Health Department of Jiangsu Province (RC2007041). We gratefully acknowledge Professors Ji-Nan Zhang and Di Yang, as well as the University of Science and Technology of China, for their assistance with the confocal microscopy.

REFERENCES

Beardslee MA, Laing JG, Beyer EC, Saffitz JE (1998). Rapid turnover of connexin43 in the adult rat heart. Circ. Res. 83(6):629-635.

Betsuyaku T, Kanno S, Lerner DL, Schuessler RB, Saffitz JE, Yamada KA, (2004). Spontaneous and inducible ventricular arrhythmias after myocardial infarction in mice. Cardiovasc. Pathol. 13(3):156-164.

Ciaccio EJ (2000). Localization of the slow conduction zone during reentrant ventricular tachycardia. Circulation 102(4):464-469.

Cottrell GT, Wu Y, Burt JM (2001). Functional characteristics of heteromeric Cx40-Cx43 gap junction channel formation. Cell. Commun. Adhes. 8(4-6):193-197.

Ek-Vitorin JF, King TJ, Heyman NS, Lampe PD, Burt J (2006). MSelectivity of connexin 43 channels is regulated through protein kinase C-dependent phosphorylation. Circ. Res. 98(12):1498-1505.

Ferreira-Cornwell MC, Luo Y, Narula N, Lenox JM, Lieberman M, Radice GL (2002). Remodeling the intercalated disc leads to cardiomyopathy in mice misexpressing cadherins in the heart. J. Cell. Sci. 115(Pt 8):1623-1634.

Fujio Y, Yamada-Honda F, Sato N, Funai H, Wada A, Awata N (1995). Disruption of cell-cell adhesion in an inbred strain of hereditary cardiomyopathic hamster (Bio 14.6). Cardiovasc. Res. 30(6):899-904.

Gutstein DE, Morley GE, Tamaddon H, Vaidya D, Schneider MD, Chen J (2001). Conduction slowing and sudden arrhythmic death in mice with cardiac-restricted inactivation of connexin43. Circ. Res. 88(3):333-339.

Harris AL (2007). Connexin channel permeability to cytoplasmic molecules. Prog. Biophys. Mol. Biol. 94(1-2):120-143.

Hertig CM, Butz S, Koch S, Eppenberger-Eberhardt M, Kemler R, Eppenberger HM (1996). N-cadherin in adult rat cardiomyocytes in culture. I. Functional role of N-cadherin and impairment of cell-cell contact by a truncated N-cadherin mutant. J. Cell. Sci. 109(Pt 1):1-10.

Johnson CM, Kanter EM, Green KG, Laing JG, Betsuyaku T, Beyer EC (2002). Redistribution of connexin45 in gap junctions of connexin43-deficient hearts. Cardiovasc. Res. 53(4):921-935.

Kamei K, Maehara K, Kimura J, Ishibashi T, Maruyama Y (2007). Comprehensive analyses of arrhythmogenic substrates and vulnerability to ventricular tachycardia in left ventricular hypertrophy in salt-sensitive hypertensive rats. Circ. J. 71(3):390-396.

Kaplan SR, Gard JJ, Protonotarios N, Tsatsopoulou A, Spiliopoulou C, Anastasakis A (2004). Remodeling of myocyte gap junctions in arrhythmogenic right ventricular cardiomyopathy due to a deletion in plakoglobin (Naxos disease). Heart Rhythm 1(1):3-11.

Kostetskii I, Li J, Xiong Y, Zhou R, Ferrari VA, Patel VV (2005). Induced deletion of the N-cadherin gene in the heart leads to dissolution of the intercalated disc structure. Circ. Res. 96(3):346-354.

Koutsouki E, Lam RS, Seebohm G, Ureche ON, Ureche L, Baltaev R (2007). Modulation of human Kv1.5 channel kinetics by N-cadherin. Biochem. Biophys. Res. Commun. 363(1):18-23.

Lerner DL, Yamada KA, Schuessler RB, Saffitz JE (2000). Accelerated onset and increased incidence of ventricular arrhythmias induced by ischemia in Cx43-deficient mice. Circulation 101(5):547-552.

Li J, Levin MD, Xiong Y, Petrenko N, Patel VV, Radice GL (2008). N-cadherin haploinsufficiency affects cardiac gap junctions and arrhythmic susceptibility. J. Mol. Cell. Cardiol. 44(3):597-606.

Li J, Patel VV, Radice GL (2006). Dysregulation of cell adhesion proteins and cardiac arrhythmogenesis. Clin. Med. Res. 4(1):42-52.

Luque EA, Veenstra RD, Beyer EC, Lemanski LF (1994). Localization and distribution of gap junctions in normal and cardiomyopathic hamster heart. J. Morphol. 222(2):203-213.

Nakao S, Platek A, Hirano S, Takeichi M (2008). Contact-dependent promotion of cell migration by the OL-protocadherin-Nap1 interaction. J. Cell. Biol. 182(2):395-410.

Noorman M, van der Heyden MA, van Veen TA, Cox MG, Hauer RN, de Bakker JM (2009). Cardiac cell-cell junctions in health and disease: Electrical versus mechanical coupling. J. Mol. Cell. Cardiol. 47(1):23-31.

Piccoli G, Rutishauser U, Bruses JL (2004). N-cadherin juxtamembrane domain modulates voltage-gated Ca2+ current via RhoA GTPase and Rho-associated kinase. J. Neurosci. 24(48):10918-10923.

Pilichou K, Nava A, Basso C, Beffagna G, Bauce B, Lorenzon A (2006). Mutations in desmoglein-2 gene are associated with arrhythmogenic right ventricular cardiomyopathy. Circulation 113(9):1171-1179.

Poelzing S, Rosenbaum DS (2004). Altered connexin43 expression produces arrhythmia substrate in heart failure. Am. J. Physiol. Heart Circ. Physiol. 287(4):H1762-1770.

Sato T, Ohkusa T, Honjo H, Suzuki S, Yoshida MA, Ishiguro YS (2008). Altered expression of connexin43 contributes to the arrhythmogenic substrate during the development of heart failure in cardiomyopathic hamster. Am. J. Physiol. Heart. Circ. Physiol. 294(3):H1164-1173.

Segretain D, Falk MM (2004). Regulation of connexin biosynthesis, assembly, gap junction formation, and removal. Biochim. Biophys. Acta 1662(1-2):3-21.

Sohl G, Willecke K (2004). Gap junctions and the connexin protein family. Cardiovasc. Res. 62(2):228-232.

Thomas G, Killeen MJ, Grace AA, Huang CL (2008). Pharmacological separation of early afterdepolarizations from arrhythmogenic substrate in DeltaKPQ Scn5a murine hearts modelling human long QT 3 syndrome. Acta. Physiol. (Oxf). 192(4):505-517.

van den Borne SW, Narula J, Voncken JW, Lijnen PM, Vervoort-Peters HT, Dahlmans VE (2008). Defective intercellular adhesion complex in myocardium predisposes to infarct rupture in humans. J. Am. Coll. Cardiol. 51(22):2184-2192.

van Rijen HV, Eckardt D, Degen J, Theis M, Ott T, Willecke K (2004). Slow conduction and enhanced anisotropy increase the propensity for ventricular tachyarrhythmias in adult mice with induced deletion of connexin43. Circulation 109(8):1048-1055.

Zhu H, Wang H, Zhang X, Hou X, Cao K, Zou J (2010). Inhibiting N-cadherin-mediated adhesion affects gap junction communication in isolated rat hearts. Mol. Cells 30(3):193-200.